FP-Experiment

Water and solute transport in porous media

Hans-Jörg Vogel and Kurt Roth
Institut für Umweltphysik

Contents

1 Overview

Background: Porous media are part of our daily life and include technical devices like filter materials and fuel cells as well as natural systems like geologic formations and soils. An important characteristic of porous media are capillary forces that play a dominant role for the dynamics of such materials. It is a challenge for physicists to model fluid flow and transport of dissolved chemicals in porous media to predict the behavior of a system as response to various boundary conditions or to construct porous media with the properties desired. The focus here is on soil, which is typically characterized by a complex structure. It consists of minerals, organic material and the pore space in-between. Moreover, this structure is typically not static but continuously changed by plants, animals and various physical boundary conditions due to temperature and precipitation. Crucial questions that require a quantitative understanding of the processes in porous media are: How to store infiltrating water in soil to warrant the growth of plants? How to prevent pollution in the environment of waste disposals? How to treat soils contaminated by anthropogenic wastes? What is the role of soils for global mass and energy fluxes?

Subject of the course: In principle, the microscopic structure of the pore space determines the behavior of porous media. However we are typically not in the position to describe this 3-dimensional structure in all detail. We aim at modeling and predicting fluid flow and solute transport in porous media at a scale of some 10^{-1}m within a soil up to some 10^3m within a catchment. This range of scales is significantly larger than the typical size of pores in soil that are in the range of 10^{-6} to 10^{-3} m. (Just think about the amount of computer memory you would need to store the structure of 1 dm^3 soil at a resolution of 1 μm). This leads to the introduction of 'effective' models based on 'effective' material properties that translate the effects of the microscopic structure into macroscopic properties.

In the first part of this course we only consider water flow in porous media and we introduce two effective material properties: 1) The relation between the energy density of water (capillary pressure) and the water saturation which is referred to as **water characteristic** and the relation between the water saturation of the media and its hydraulic conductivity which is termed the **hydraulic conductivity function**. An experiment is performed to determine these basic material properties which are essential for modeling the dynamics of fluids in porous media at larger scales.

In the second part we consider solute transport through porous media which also may be related to macroscopic material properties as for instance a dispersion tensor. Another experiment is performed to identify a convenient **transport model** and to determine the related parameters.

Preparation   To prepare this course, this short script should be sufficient. Here, the basic theory of water dynamics in porous media is described and some practical details on the set-up of the experiment are provided. Finally the evaluation of the measured data through inverse modeling is described. At least the theoretical part should be worked through prior to the course. For a deeper study of the subject you may consider PartI and PartII-1 of *Lecture Notes in Soil Physics* [*Roth*, 1996] at www.iup.uni-heidelberg.de/institut/forschung/groups/ts/students/edumat.html

2 Part I: Estimation of hydraulic properties by inverse modeling

2.1 Introduction

To model the dynamics of water in porous media at a scale much larger than the individual pores, we introduce so called "effective material properties" which are based on variables that are visible at the larger scale. These properties and the related variables are obtained by averaging over the complicated porous structure at the microscopic scale. Thereby, the details of the porous structure are lost, but the aim is to preserve those properties that are important to quantitatively understand the processes at the larger scale – this is why we call them 'effective'. A simple example is the transition from the detailed binary structure of single pores to a continuous variable at the large scale, i.e. the porosity, which measures the fraction of pores per unit volume. This is illustrated in figure 1.
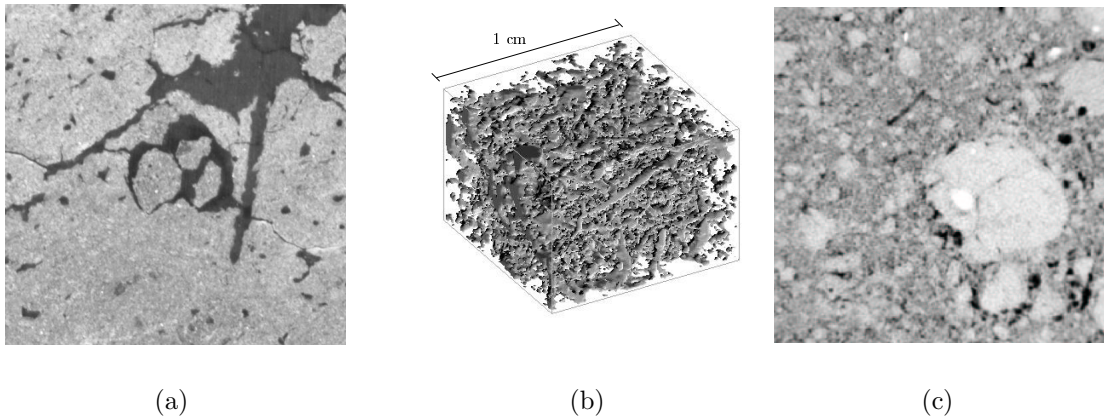

(a) (b) (c)

Figure 1: *2D and 3D structure of soil at the pore scale with a resolution of 0.04 mm/pixel obtained from serial sections (a and b). Structure of porosity including few large pores (black spots) at a larger scale with a resolution of 0.4 mm/pixel obtained by X-ray tomography (c).*

At the pore scale (Figure 1 b), flow and transport processes may be described using classical concepts of fluid dynamics where the acceleration of a fluid element is related to the forces acting on it, most importantly to gravity, pressure gradients and friction. This leads to the well-known Navier-Stokes equation. This equation is not invoked here, however, because (i) the inertial term can be neglected for the low flow velocities typically encountered and (ii) implementing the boundary conditions for the pore space is next to impossible. Instead, we go for a continuum description that is obtained from averaging. In formal analogy to the averaging used in thermodynamics, the dynamics of water flow is described over a representative region of the pore space. The remaining task then, is to estimate pertinent effective material properties.

2.2 Theory

2.2.1 Dynamics of Water Movement

As a first step towards a quantitative description of water flow in porous media we formulate the conservation of mass of water – actually of volume since water may be considered as incompressible – as

$$\partial_t \theta + \nabla \cdot \mathbf{j}_w = 0 \; , \tag{1}$$

where θ is the volumetric water content and $\mathbf{j}_w$ [L T^{-1}] the volume flux of water. In the following, we call $\mathbf{j}_w$ the water flux, and assume that it is linearly related to the gradient of the potential energy density ψ_w of the water. We call ψ_w the water potential. It will be discussed further down. The flux law thus is of the form

$$\mathbf{j}_w = -\mathsf{K}(\theta)\nabla\psi_w \; , \tag{2}$$

where the tensorial quantity $\mathsf{K}(\theta)$ is the hydraulic conductivity that depends on the volumetric water content. This is called the *Buckingham-Darcy law*. Notice the formal analogy with flux laws for heat (Fourier), dissolved substances (Fick), and electric charge (Ohm).

Inserting the flux law into the conservation equation yields the *Richards equation*

$$\partial_t \theta - \nabla \cdot [\mathsf{K}(\theta)\nabla\psi_w] = 0 \tag{3}$$

for the dynamics of water movement. Obviously, this equation cannot be solved yet because there occur two unknowns, θ and ψ_w. We will find in the next section, that there exists a relation between θ and a component of ψ_w, the matric potential ψ_m which accounts for surface forces (capillary forces). This relation, which is called the soil water characteristic $\theta(\psi_m)$, turns out to be a material property of the porous material as is the hydraulic conductivity $\mathsf{K}(\theta)$.

2.2.2 Material properties and state variables

The complicated structure of the soil cube in Figure 1b is replaced by 'effective' measures and state variables with respect to the fluids. This can be interpreted as *averaging* over microscopic properties or *upscaling* from microscopic to macroscopic properties.

For the pore structure which we assume to be rigid we introduce the constant material properties

- **porosity** ϕ [-], the volume fraction of pores

- **water characteristic** $\theta(\psi)$ the relation between water content and water potential

- **saturated hydraulic conductivity** K_s [m s^{-1}], in case all pores are filled with water

With respect to the fluid (in our case water) within the pore space we introduce the state variables

- **volumetric water content** θ [-], the volume fraction of water filled pores,

- **energy density of the water or water potential** ψ_w [J m^{-3}], which includes, in a first approximation, gravity and capillary forces.

All these quantities may be attributed to a given volume of soil which is large enough to contain all the microscopic heterogeneities. We call such a volume a *representative elementary volume* (REV). From the definitions given above we can already find some basic relations for a soil sample of volume V_0. Obviously, within the 3-phase system **s**olid-**w**ater-**a**ir we find $V_0 = V_s + V_w + V_a$ with the porosity $\phi = (V_w + V_a)/V_0$ and the water content $\theta = V_w/V_0$. The water content at complete water saturation ($V_a = 0$) correspond to the porosity $\theta_s = \phi$. If we know the density of the solid material ρ_s (for quartz it is 2.65 g/cm^3) we can calculate the porosity from bulk density $\phi = 1 - (\rho_b/\rho_s)$.

In the 3-phase system soil, the hydraulic conductivity K is clearly not a material constant because the conductivity depends on the water content. This is in contrast to groundwater where $\theta = \theta_s$ is constant. In soil however, the water content is a state variable that may vary and herewith also the hydraulic conductivity. With decreasing water content the overall cross section that conducts water decreases, as well as the size of the water filled pores and additionally, the water has to bypass air filled pores. All together this leads to a nonlinear decrease of K with θ. Hence, the function $K(\theta)$ is the material property (see below).

Besides the water content, the other relevant state variable of the 3-phase system that varies in space and time is the energy density of water ψ_w, in the following referred to as **water potential**. At a given location in the soil, this is the energy per unit volume of water, which is required to bring water from a reference state to that location. We consider the reference state as free water at some defined height z_0. In the simplest case, the total water potential ψ_w is composed of only two components: the potential due to gravity, ψ_g, and the so called matric potential ψ_m which includes the effect of capillary forces. We choose the z-axis to be positive downward and write

$$\psi_w = -\rho_w g[z - z_0] + \psi_m \ , \tag{4}$$

where ρ_w is the density of water and g the acceleration due to gravity.

The meaning of ψ_g is immediately clear but what about the matric potential ψ_m? In unsaturated porous media, this potential describes the energy densities associated with the boundary layers solid-liquid and liquid-gas. In mineral soil, the solid soil matrix is typically wettable so that the solid material is completely covered by a water film (i.e. the energy density of the boundary layer solid-liquid is smaller that that of liquid-gas). Hence, the matric potential ψ_m is only determined by the interface liquid-gas.

Our experiments are restricted to high water contents where the liquid-gas interface has a constant energy density which is the surface tension σ_{wa} (0.0725 J m^{-2} for pure water at 20°C). At equilibrium, when the free energy in minimal, the surface area of the liquid-gas interface is also minimal and one can show that this surface is described by the Young-Laplace Equation:

$$\psi_m = p_w - p_a = \sigma_{\text{wa}} \left[\frac{1}{r_1} + \frac{1}{r_2} \right] \ , \tag{5}$$

where p_w and p_a are the pressures in water and air, respectively, and r_1, r_2 are the principal radii of curvature. We use the convention that the sign of the radius is negative if it is within the air phase. In the simplest case of a cylindrical capillary (5) reduces to $\psi_m = p_w - p_a = 2\sigma_{\text{wa}}/r$.

There are a few important implications:

- The energy density [J m^{-3}] equals the pressure jump across the interface [N m^{-2}]

- In equilibrium, r is constant for constant depth

- Water in wettable porous media tends to fill the small pores (maximizing r) while air reside in the large pores.

Consequently, there must be a relation between the volumetric water content θ and the curvature of the minimal interfaces and herewith ψ_m. This relation $\theta(\psi)$ is illustrated in figure 2: with decreasing water content, the water retreats to smaller pores and the matric potential ψ_m becomes more negative.
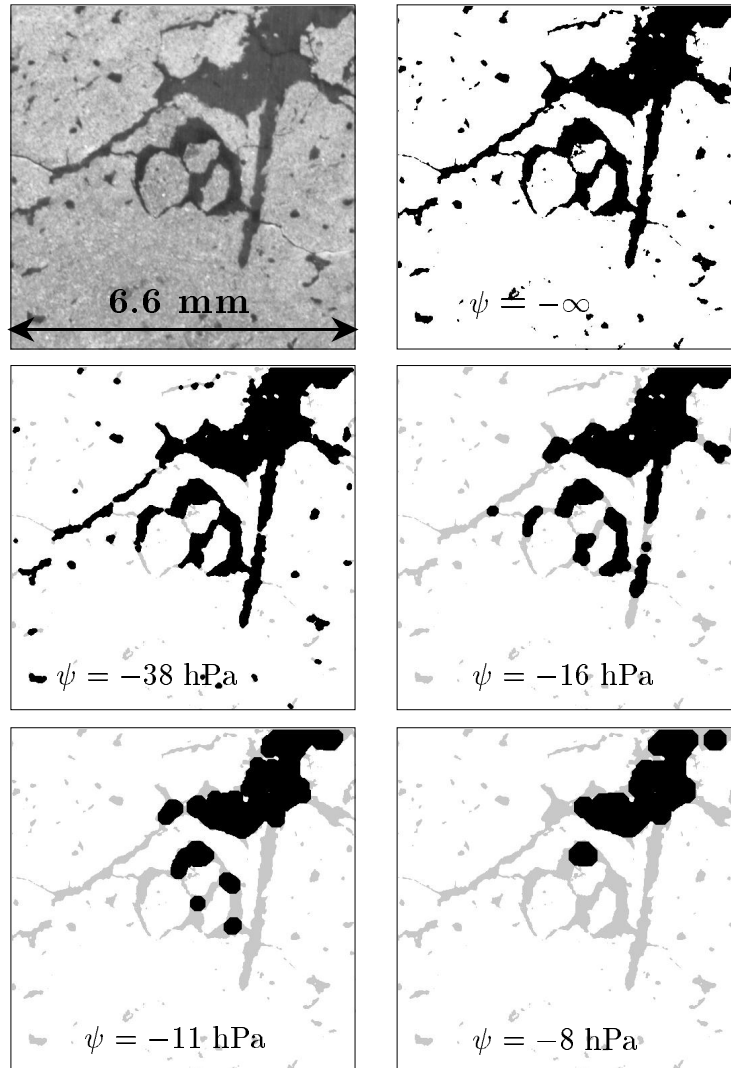

Figure 2: *Distribution of different phases (water: grey, air: black) within a 2D section through a porous media at different matric potentials ψ_m. Note the different radii of curvature of the interfaces according to the Young-Laplace equation (5).*

We note that in many applications - and also in this course - the equivalent height of a water column h_i [cmWC] is used instead of the potential ψ_i with

$$h_i := \frac{\psi_i}{\rho_w g} \qquad (6)$$

$(1 \ \mathrm{cmWC} \approx 1 \ \mathrm{hPa} = 1 \ \mathrm{mbar})$.

Additional remarks:

1. *We restrict the description of the matric potential to the most simple case. In reality the situation is much more complicated. In particular, σ_{wa} is not a constant but depends on temperature and on the composition of the water phase (dissolved chemicals). Moreover, the wettability of soil may vary in time and space. Finally, σ_{wa} changes with the thickness of the water layer when going to very dry conditions.*

2. *We assume that there is an instantaneous equilibrium between θ and ψ_m which is only the case at high water contents and herewith small resistivity to water flow. In the dry range however, water in adsorbed films is barely mobile and equilibration has to be reached through vapor diffusion which is a very slow process.*

3. *Besides gravity and capillarity, there may be additional forces: osmotic forces due to gradients in salt concentration, mechanical forces in case the solid material is deformable (this is the rule especially in clay rich soils), and the air pressure may be locally increased when air is entrapped by the water phase.*

2.2.3 Hydraulic properties

In the previous sections we have seen that we require two different relations for an effective description of the porous medium at a larger scale: the **hydraulic conductivity function** $K(\theta)$ and the relation between water content and matric potential, which we term **soil water characteristic** $\theta(\psi)$.
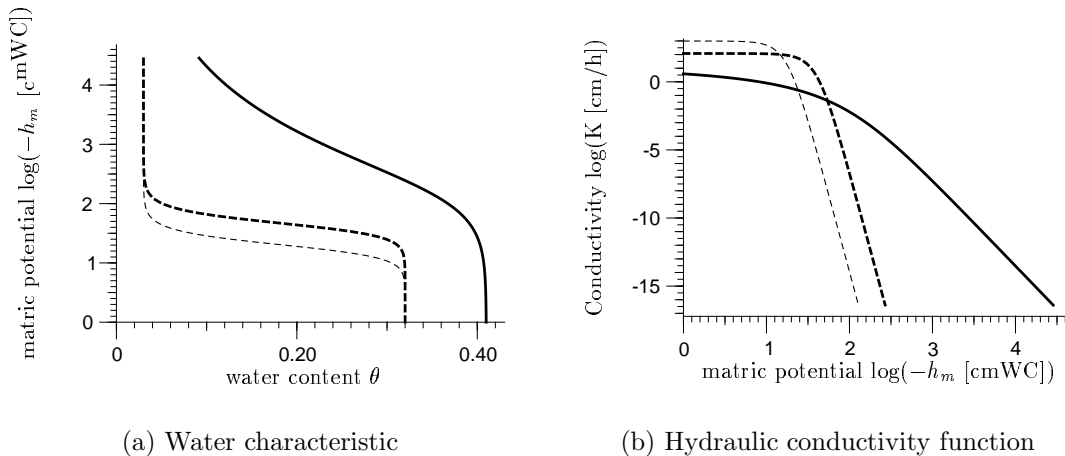

(a) Water characteristic

(b) Hydraulic conductivity function

Figure 3: *Typical hydraulic properties of a loamy soil (solid line) and a sandy soil (dashed line). The thin dashed line represents a sand with larger grains and thus, larger pores.*

Soil water characteristic

Figure 3 shows typical examples for a loamy and a sandy soil. The loamy soil has a higher water content at saturation, θ_s, because of a higher porosity. Going from complete saturation to dryer conditions by lowering the matric potential the water content of the sandy material decreases very rapidly below a potential of $h_m \approx -30$ cmWC. This is because this sand is a rather homogeneous material where all pores are within a narrow size range. According to the Young-Laplace equation (5) and using (6) we find an equivalent pore radius for $h_m = -30$ cmWC of $r \approx 0.05$

mm. When going from -30 cmWC to about -100 cmWC the water within these pores is removed. In the loamy soil the water content decreases more continuously with decreasing water potential, meaning that the size distribution of pores is much broader compared to the sand. Clearly, the shape of the soil water characteristic is an effective description of the underlying pore structure. However, it should be noted that not only the size distribution of pores determines the shape of $\theta(\psi)$ but also the connectivity of the pores. The complicated connectivity of pores in soil also leads to the phenomenon of hysteresis. Both effects are illustrated in Figure 4.
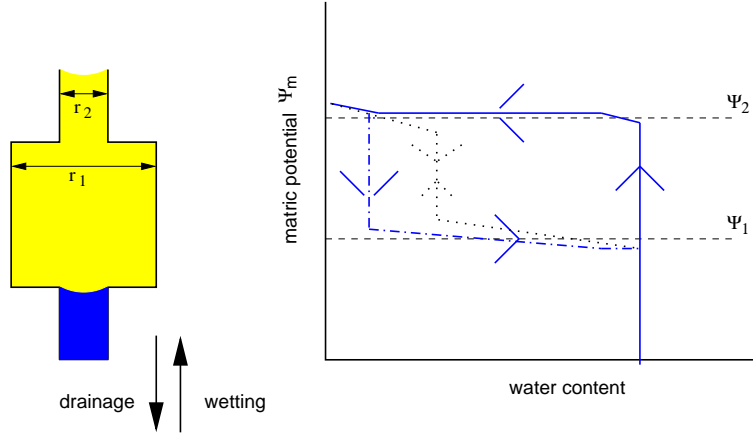

Figure 4: *Effect of pore connectivity on the hysteretic behavior of the water characteristic shown for an idealized pore: at $\psi_1 < \psi_m < \psi_2$ we can find very different water contents during drainage (light grey) and wetting (dark grey) at the same matric potential (same interface radius). Without the effect of connectivity (in case of parallel capillaries) we would find the non-hysteretic dotted line.*

The water characteristic is often described by the parameterization of van Genuchten which can be fitted to a wide range of different materials:

$$\Theta(\psi) = \frac{\theta - \theta_r}{\theta_s - \theta_r} = [1 + [\alpha\psi]^n]^{-1+1/n} \tag{7}$$

with the parameters
Θ [-]   water saturation $[0, 1]$
θ_s [-]   water content at saturation
θ_r [-]   residual water content
α [cm^{-1}]   empirical parameter
n [-]   empirical parameter
The residual water content θ_r represents the small amount of water which is adsorbed in thin films at low water potentials and which is barely mobile (see Fig. 3 for $\log(-\psi_m) > 3$ in the sand). The parameter α scales h_m and thus determines the position of the curve relative to the axis of matric potential and the parameter n determines the shape of the curve. Thus, α is related to the mean pore size and n to the width of the pore size distribution. However both parameters are fitting parameters without immediate physical meaning. The parameters for the curves in Figure 3 are give in Table 1.

Hydraulic conductivity function

In Figure 3 the hydraulic conductivity functions $K(\psi_m)$ are shown for the sandy and the loamy soil. Although the porosity of the sand is lower, the hydraulic conductivity at water saturation is higher in the sand. This is because the pores are larger (see $\theta(\psi)$). However, for decreasing water potential the conductivity in the sand drops very rapidly. This is intuitively clear, because at the critical water potential below $h_m \approx -30$ cmWC also the water content drops significantly. Hence, the shape of $\theta(\psi)$ tells us something about the shape of $K(\psi)$ which is also used for the parameterization. Using arguments derived from statistical pore models *Mualem* [1976] proposed to derive the hydraulic conductivity curve through integration of the water characteristic

$$K(\Theta) = K_0 \Theta^\tau \left[\frac{\int_0^\Theta \psi^{-1} d\Theta}{\int_0^1 \psi^{-1} d\Theta} \right]^2 \qquad (8)$$

Inserting the van Genuchten parameterization (7) this leads to

$$K(\Theta) = K_0 \Theta^\tau \left[1 - [1 - \Theta^{n/[n-1]}]^{1-1/n} \right]^2 \qquad (9)$$

where now the conductivity is given as a function of Θ. Note that the shape of the curve is determined by the same shape parameter n as for the soil water characteristic. The hydraulic conductivity at water saturation, K_0 is introduced as a parameter to fix the absolute height of the hydraulic conductivity. Moreover an additional parameter, τ, is used which is termed 'tortuosity' and which is thought to account for the change in the topology of the water phase with decreasing water content. However, τ is considered to be a pure fitting parameter which frequently is fixed at a value of 0.5.

At this point we arrive at the complete set of hydraulic parameters, describing the hydraulic properties of porous media. These parameters are listed in Table 1 for the examples shown in Figure 3. The aim of the first part of this course is to experimentally determine such a parameter set for a given soil.

Table 1: van Genuchten/Mualem parameters of the hydraulic functions shown in Figure 3

Parameter		Sand (fine)	Sand (coarse)	Silt
α	$[\text{m}^{-1}]$	2.3	5.3	0.7
n		4.17	4.17	1.3
θ_r		0.03	0.03	0.01
θ_s		0.32	0.32	0.41
τ		0.5	0.5	0.5
K_0	$[10^{-5} \text{ m s}^{-1}]$	2.2	5.5	1.0

2.2.4 Experimental determination of hydraulic properties by inverse modeling

Direct measurements of hydraulic properties are very time consuming and, in case of hydraulic conductivity, also very difficult. In this practical course, we apply an indirect method, the approach of inverse modeling, which is based on the theory given in the previous chapter.

The basic idea is that we can describe the dynamics of the system through Richards equation (3). Thus, for a given set of initial and boundary conditions, we can predict the behavior of the system in case the hydraulic properties are known - which is not the case here. But we can observe the behavior of the system and choose the hydraulic properties such that they explain our observation. This approach is called inverse modeling. This is in contrast to the classical direct problem: Given the material properties, the initial and boundary conditions and a convenient model we solve for the dynamic behavior. Here, we face the inverse problem: Given the initial and boundary conditions, a convenient model and the system dynamics we solve for the material properties

In particular, the soil sample is excited by applying different pressures to the water phase at the lower boundary of the sample and we measure the induced water flow over that boundary and the matric potential of the water at some point within the soil. Then, Richards equation is solved to simulate these fluxes and potentials. Thereby we start with a first guess of starting values for the hydraulic parameters (Table 1). Subsequently, these parameters are changed iteratively to minimize the difference between experimental results and the simulation which finally leads to the determination of the parameters. In that way, all parameters are estimated consistently for one single experiment.

2.3   Experiment

2.3.1   Setup of the experiment

Figure 5 shows a sketch of the experimental set up for a so called 'mulitstep-outflow' experiment:

- The soil sample is mounted on a porous plate which is completely saturated with water. The pores of this plate are small enough to stay water saturated in the range of pressures applied during the experiment. Thus, the plate is only permeable for water not for gas. In this way we connect the soil water to an outer water reservoir the pressure of which can be controlled.

- A pressure sensor (DS1) is installed at the porous plate.

- A tensiometer with pressure sensor (DS3) is installed in 2 cm depth to measure the matric potential during the experiment.

- The water outflow is collected in a burette. The water level in the burette can be measure by another pressure sensor (DS2).

- The pressure at the porous plate can be controlled by a computer through 2 magnetic valves (V1, V2) which are connected to a pressure reservoir and the atmosphere respectively.

2.3.2   Example

Figure 6 shows typical results obtained by a multistep-outflow experiment:

- Exciting the system:
  Dashed line   pressure at the porous plate (lower boundary condition) as controlled by the computer to excite the system.

- System response:
  Triangles   pressure at the tensiometer (DS3).
  Circles   water level in the burette (DS2).

- Parameter estimation:
  Thick line   solution of Richards Equation for the water dynamics (flow into the burette and back to the soil) for the given boundary conditions and a hypothetical set of hydraulic parameters.
  Thin line   corresponding solution of Richards Equation for the pressure at the tensiometer.
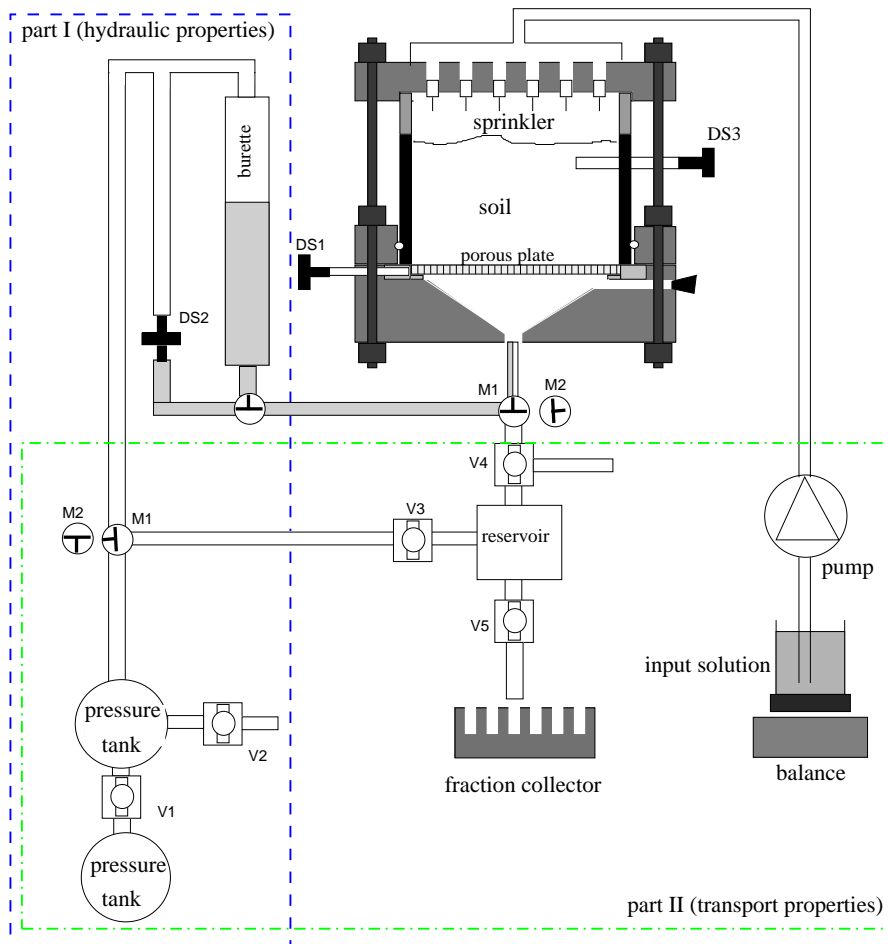
Figure 5: *Sketch of the experimental set up*

2.3.3   Schedule of the practical course (part I)

First day:

1. Introduction

2. Calibration of pressure sensors

3. Installation of the tensiometer and all pressure sensors

4. Installation of magnetic valves.

5. Saturation of the sample with water.

6. Quality assurance of the sensors' output

7. Estimation of optimal boundary conditions (pressure steps) based on estimated pore size distribution using Young-Laplace equation.

8. Configuration of the boundary conditions

9. Start of the experiment which runs over the night.
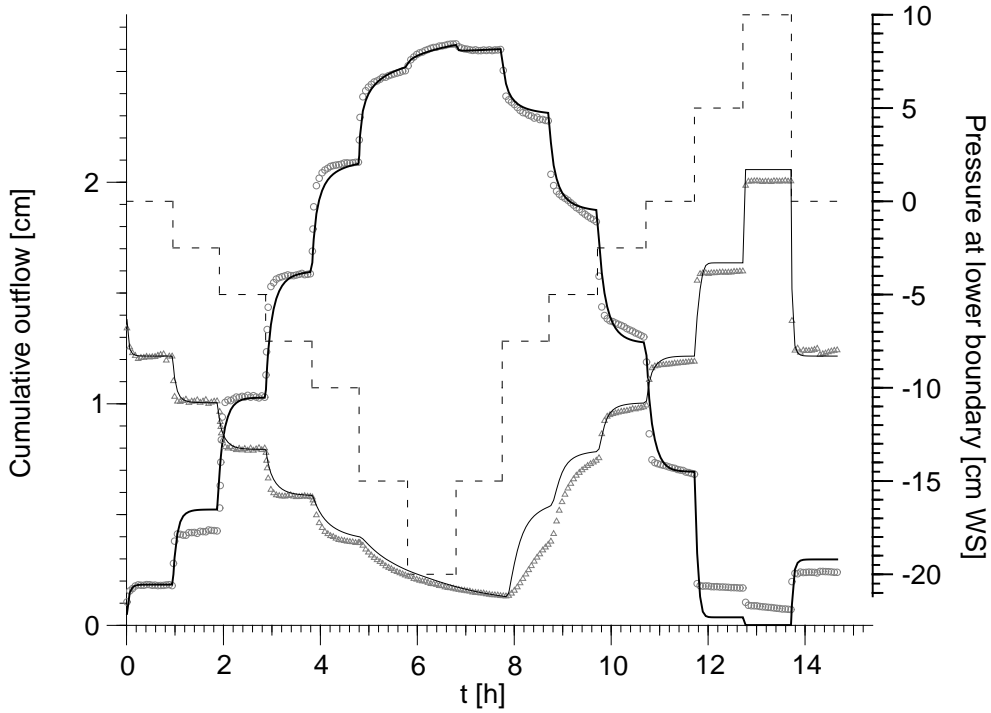
Second day:

Figure 6: *Typical results of a multistep outflow experiment*

1. End of the Experiment.

2. Introduction to the parameterization of hydraulic material properties.

3. Parameter estimation 'by hand'. A computer program is provided that solves Richards equation for a given set of hydraulic parameters and the specified initial and boundary conditions. Starting with a first guess (parameters for sand in Tab. 1), the parameters are changed such that the difference between experimental results and simulations is minimized.

4. Parameter optimization using Levenberg-Marquardt algorithm for non-linear regression. Thereby, the squared sum

$$\chi^2 = \sum_{i=1}^{N} \left[\frac{y_i - f_i(\eta)}{\sigma_i} \right]^2$$

of deviations between experiment and simulation is minimized, where y_i is the measurement i and $f_i(\eta)$ is the expected result based on the parameter vector $\eta(\theta_s, \theta_r, \alpha, n, \tau, K_s)$ and σ_i is the estimated variance for the measurement at point i.

5. Critical discussion of the quality of the results: Confidence intervals and correlations of the parameters, error sources.

2.4 What to learn in this experiment

1. The concept of effective properties of a complex object (soil) which cannot be described in any detail.

2. Fundamentals of inverse modeling, i.e. regression, where the fitted model is not a simple functional relation but requires the numerical solution of a partial differential equation.

3. Application of electronically controlled devices.

2.5   Questions you should be able to answer before starting

1. What is hydraulic conductivity? How qualitatively does it depend on water content?

2. What is matric potential? What is its physical basis?

3. What is the soil water characteristic function and what is its general form? Why?

4. What is the origin of the hysteresis of $\theta(\psi_m)$?

5. How does the multi-step outflow measurement work?

3 Part II: Measurement and parameterization of solute transport

3.1 Introduction

As we have seen in the first part, the hydraulic properties of porous media together with Richards' Equation provide the basis for modeling the dynamics of fluids in porous media. Given this dynamics what can we say about the transport of dissolved chemicals?

We consider conservative solutes, meaning dissolved chemicals that do not interact with the solid phase through sorption or any reaction. For such chemicals the mean transport velocity can be calculated from the water flux j_w which may be obtained as a result of Richards' Equation.

However, in many circumstances we are not only interested in the mean velocity of solutes but especially in the highest or the lowest velocities. These extreme values are related to questions like: When will the first percent of some contaminant reach the groundwater? or, how long does it take to remove some resident contamination from a porous medium?

It is evident from the heterogeneous structure of most porous media (see Figure 1) that the velocity field encountered at the pore scale is heterogeneous as well. There may be a wide range of velocities due to the different size and different continuity of pores. As a consequence, solute transport in porous media is typically characterized by significant dispersion processes. Thus, an originally sharp solute pulse is blurred by the wide spectrum of microscopic velocities in addition to molecular diffusion. This process is referred to as *hydrodynamic dispersion*. The aim of this part is to measure and model the dispersion of a solute pulse for a transport experiment in a soil column.

3.2 Theory

3.2.1 Convection-Dispersion model (CD)

We start from the consideration of a heterogeneous velocity field within the pore space of a porous medium as illustrated in Fig. 7, and we look at the fate of a set of particles which enter this velocity field somewhere at the boundary z_0 at time t_0.

The particles move according to the streamlines of the velocity field and after some time Δt they reach the location Δz with mean $\langle z \rangle$ and variance σ_z^2 due to the different velocities. In an initial stage of this process it is likely that the particles retain the velocity which they encountered at the beginning. Consequently, we would expect that the variance of transport distances will increase with time according to the heterogeneity of the flow field.

In a later stage, we assume that each particle may change its velocity when moving from one streamline to another through molecular diffusion. Thus, in the limit of long travel times, each particle has explored all different velocities within the porous medium. Then, according to the *central limit theorem* (CLT), the distribution of travel distances approaches a Gaussian distribution with a given mean and variance. Thereby, the mean $\langle z \rangle = \bar{V} t$ depends on the mean velocity $\bar{V}$ which can be calculated from the water flux

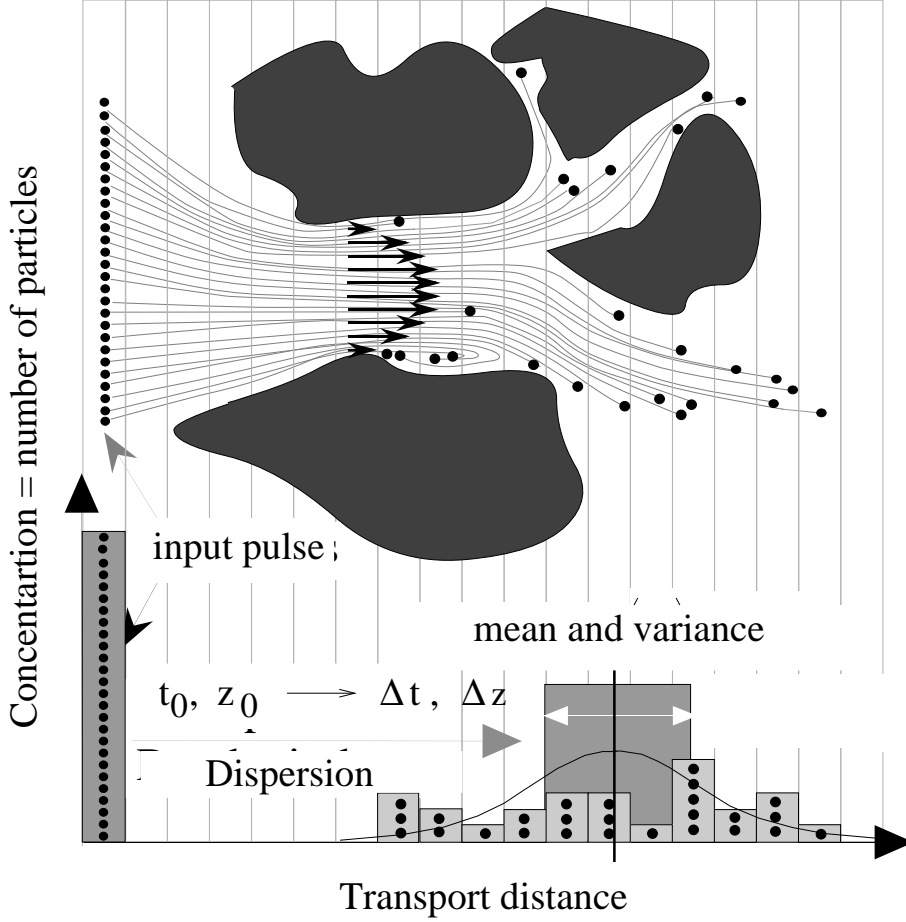$$\bar{V} = \frac{j_w}{\theta} \, ,$$

$$(10)$$

Figure 7: *Dispersion of a solute pulse through a heterogeneous velocity field*

and the variance is a result of hydrodynamic dispersion and molecular diffusion.
This is the basic idea for the convection-dispersion model (CD) where we distinguish between a convective and a dispersive component of solute transport. The convective solute flux j_s^{conv} [M L^{-2} T^{-1}] is determined by the water flux:

$$j_s^{\text{conv}} = j_w c_w \; , \tag{11}$$

where c_w is the solute concentration in the water phase. The dispersive component j_s^{disp} is described in analogy to a diffusion process:

$$j_s^{\text{disp}} = -D_{\text{eff}} \frac{\partial}{\partial z} c_w \; , \tag{12}$$

where D_{eff} is an effective diffusion coefficient which comprises all dispersion processes including molecular diffusion and hydrodynamic dispersion. This formulation is motivated by the insight, that hydrodynamic dispersion as well as molecular diffusion leads to a Gaussian solute distribution. From (11) and (12) we obtain the total solute flux as

$$j_s = j_s^{\text{conv}} + j_s^{\text{disp}} = j_w c_w - D_{\text{eff}} \frac{\partial}{\partial z} c_w \; . \tag{13}$$

To arrive at a complete description of solute transport we formulate the mass balance

$$\frac{\partial}{\partial t} \theta c_w + \frac{\partial}{\partial z} j_s = 0 \; , \tag{14}$$

16

and we insert the flux law (13) to get the *convection dispersion equation* (CDE):

$$\frac{\partial}{\partial t}\theta c_w + \frac{\partial}{\partial z}\left[j_w c_w - D_{\text{eff}}\frac{\partial}{\partial z}c_w\right] = 0 \ , \tag{15}$$

We can simplify this equation by inserting the convective velocity (10) and by replacing the effective dispersion coefficient by $D := D_{\text{eff}}/\theta$. Then, assuming constant water content θ, we get

$$\frac{\partial}{\partial t}c_w + V\frac{\partial}{\partial z}c_w - D\frac{\partial^2}{\partial z^2}c_w = 0 \ , \tag{16}$$

with V and D as free parameters of the CD-model. Evidently, the mean travel distance of a solute pulse at a given time t is related to V and the variance of travel distances is related to D. From analytical solutions of (16) we find:

$$\langle z \rangle = Vt \ , \tag{17}$$

and

$$\text{var}(z) = 2Dt \ . \tag{18}$$

In analogy to the distribution of travel distances at a given time t, we can also analyze the distribution of travel times to a given depth z. This distribution can be measured in a classical column experiment where a solute pulse is infiltrated into the porous media by a constant water flux and the solute concentration in the outflow is measured as a function of time. Figure 8 shows the result of such a *break through curve* for a solute input in form of a concentration step. Clearly, the expectation of the travel time $\langle t \rangle$ and the variance of travel times again depend on the parameters V and D. We find

$$\langle t \rangle = \frac{z}{V} \ , \tag{19}$$

and

$$\text{var}(t) = \frac{2Dz}{V^3} \ . \tag{20}$$

Thus, we recognize, that the parameters V and D can be estimated from the first two moments of the travel distance distribution or the travel time distribution respectively.

In this practical course we will measure the break through curve of the food dye Brilliant Blue which is applied as a step input at constant water flux.

3.2.2 Extension to multi-domain models (MIM)

The CD-model described above implies that all available water is equally involved in solute transport. However, in many experiments we find that the shape of the break-through curve is not Gaussian, especially that a relatively quick break through of solute is followed by a long tail of very slow particles. Conceptually, this phenomenon can be described by separating the available water θ into two components, one, θ_{m}, which is mobile and another, θ_{im}, which is immobile. Then we obtain the so-called mobile-immobile model (MIM)

$$\frac{\partial}{\partial t}c_{\text{m}} + \frac{\theta_{\text{im}}}{\theta_{\text{m}}}\frac{\partial}{\partial t}c_{\text{im}} + V\frac{\partial}{\partial z}c_{\text{m}} - D\frac{\partial^2}{\partial z^2}c_{\text{m}} = 0 \tag{21}$$

$$\frac{\partial}{\partial t}c_{\text{im}} = -\omega[c_{\text{im}} - c_{\text{m}}] \ , \tag{22}$$

where we consider the concentration in the mobile phase only, and an additional term describing the exchange between the mobile and the immobile phase. This exchange, $\partial_t c_{im}$, is controlled by the rate parameter $\omega \in [0, \infty]$, where $\omega \to 0$ means no exchange and $\omega \to \infty$ instantaneous equilibrium between mobile and immobile phase. If $\omega > 0$ the mean velocity of the particles is reduced due to their residence time in the immobile phase. This residence time is proportional to θ/θ_m which can be defined as a retardation factor

$$R = \frac{\theta}{\theta_m} = 1 + \frac{\theta_{im}}{\theta_m} \tag{23}$$

As an extension to the classical CD model we now have the additional parameters R and ω to fit the model to measured break through curves. A typical example is shown in Figure 8. (Note that in the limit of long travel distances or long travel times, the shape of the break through curve will be identical to that of a simple CD process, however the mean velocity is reduced by the factor R).
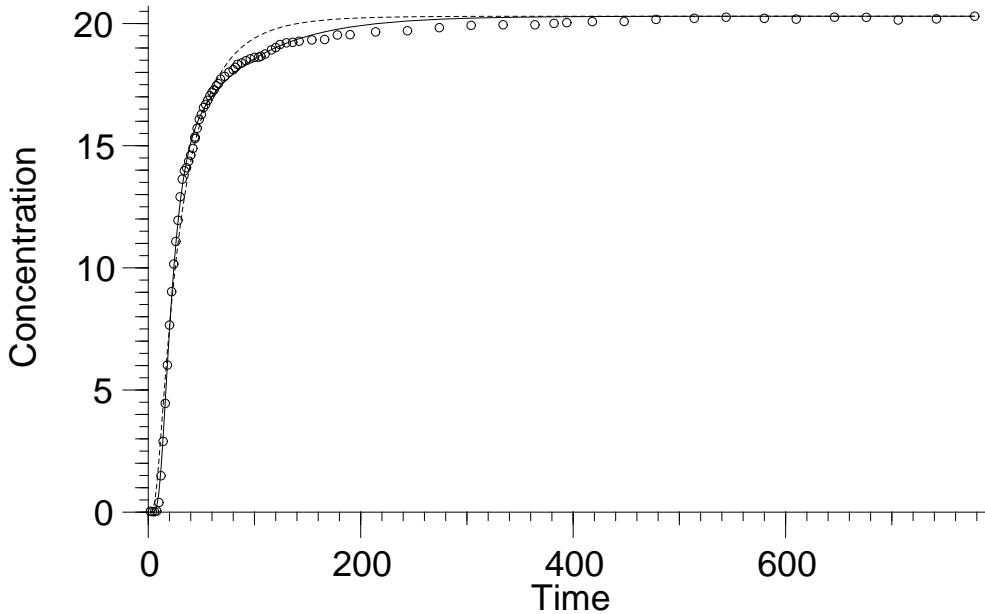

Figure 8: *Measured break through curve (symbols) together with fitted CD (dashed line) and fitted MIM-model (solid line)*

3.3   Experiment

3.3.1   Setup of the experiment

The experimental setup is shown in Figure 5. The sample stays in the same position on the ceramic plate as for the multistep outflow experiment in part I. But now the valves **M** are turned to position 2 and the water below the ceramic plate is removed. Thus, the pressure at the lower boundary is applied through the gas phase and the outflow of water is collected in a reservoir. Depending on the water flux, this reservoir is depleted from time to time into test tubes which are mounted on a fraction collector. The depletion is controlled by 3 magnetic valves: first the pressure line is interrupted (**V3**) then atmospheric pressure is let in (**V4**), finally the reservoir is depleted by opening **V5**. In this way it is possible to analyze the solute concentration in the outflow as a function of time.

At the upper boundary we install a sprinkler, which is connected to a reservoir of input solution. This reservoir is placed on a balance, so that the actual flux can be determined, and can be controlled by a pump. All devices are controlled by a computer.

3.3.2 Schedule of the practical course (part II)

First day:

1. Introduction

2. Rebuild the experimental setup: switch valves M to position 2, remove water below the ceramic plate, connect outflow tube to V4.

3. Install the fraction collector with test tubes, prepare pure water as input solution on the balance and connect the input solution through a pump with the sprinkler.

4. Before mounting the sprinkler on the column, switch on the pump at a high speed an remove all air bubbles within the tubes and the sprinkler.

5. Connect all the devices to the corresponding ports at the computer and write what you have done to the file 'instruments.dat' which is required by the control program.

6. We want to establish a stationary water flux $j_w = 5$ mm/h and we wish to have a constant matric potential ψ_m within the entire sample during the experiment. Calculate the matric potential ψ_m which is expected for the desired water flux from the hydraulic parameters obtained in part I. This potential is given as the lower boundary condition in the file 'dynamics.dat'.

7. Calculate the time interval to deplete the reservoir so that the amount of water within the reservoir will not exceed 10 ml. Add this time to the file 'dynamics.dat'.

8. Start the experiment with pure water to establish stationary flow conditions. (think about how to check if this conditions are reached).

9. Calculate the fraction time for the fraction collector so that you will get 20 ml/tube.

10. Calculate the duration of the experiment, so that the volume of water inside the sample is replaced 4 times during the experiment (you can calculate the expected water content from the hydraulic parameters obtained in part I).

11. After stationary conditions are reached, start of the experiment which runs over the night: Switch input solution to Brilliant Blue and switch on the fraction collector.

Second day:

1. End of the Experiment.

2. Collect all the tubes and analyze the dye concentration with the spectrometer.

3. Calculate velocity V and dispersion coefficient D from mean and variance of the travel time using (19) and (20).

4. Use these parameters as a first guess and optimize them by adjusting the CD model to the complete set of measured data. A computer program is provided that solves the CDE for a given set of parameters.

5. After you arrived at an optimal fit based on the CD-model use the MIM-model to see if you can get a better description of the experiment.

6. Use the Levenberg-Marquardt algorithm to get even better.

7. Critical discussion of the quality of the results: Confidence intervals and correlations of the parameters? which data are sensitive for which parameters?

3.4   What to learn in this experiment

1. The concept of effective description of solute transport within a complex object (soil) which cannot be described in any detail.

2. Estimation of control factors for an experiment based on known boundary conditions and a process model.

3. Application of electronically controlled devices.

3.5   Questions you should be able to answer before starting

1. What is the meaning of hydrodynamic dispersion in porous media?

2. Why is it a good idea to describe dispersion in analogy to diffusion?

3. What is a break through curve?

References

Mualem, Y., 1976: A new model for predicting the hydraulic conductivity of unsaturated porous media, *Water Resources Res.*, **12**, 513–522.

Roth, K., 1996: Lecture Notes in Soil Physics, *http://www.iup.uni-heidelberg.de/institut/forschung/groups/ts/students/edumat.html*, pp 142.